Archives of Hydro-Engineering and Environmental Mechanics
Vol. 49 (2002), No. 3, pp. 31–45

Turbulent Shear Stresses and Prime Velocity Distribution in Compound Channels

Włodzimierz Czernuszenko

Polish Academy of Sciences, Institute of Geophysics
Ks. Janusza 64, 01-452 Warszawa, Poland, e-mail: wczer@igf.edu.pl

(Received August 21, 2002; revised October 12, 2002)

Abstract

The turbulent stresses must be defined to calculate the velocity distributions in open channel flows. In the paper, the turbulent stresses are presented as a sum of the normal and shear turbulent stresses. The normal turbulent stresses act like pressure, i.e., they are isotropic and can be absorbed by the pressure-gradient term in the momentum equations. Therefore, only the shear stresses have to be defined to describe the velocity distribution, e.g., the prime velocity distribution in an open channel flow. The shear turbulent stresses are defined by the 3D mixing length hypothesis. This hypothesis is based on the mixing length tensor (MLT). It is shown how to define the components of MLT for compound channels and how to relate it to the turbulent stress tensor. The components of the MLT are defined based on the concept of the generic mixing length (GML). This concept is presented. Having calculated the generic mixing length, the main components of the MLT as well as the turbulent shear stresses can be calculated.

The presented concept is applied to calculate the prime velocity distribution in laboratory open channels with two-stage cross-section. Two channels are considered, one with vertical sidewalls and one with inclined sidewalls. The basic hydrodynamics equations (parabolic approximation of Reynolds equations) together with the turbulence model are solved. The well-known Patankar-Spalding algorithm was used to solve these equations. Some numerical simulations were performed for different components of MLT, i.e. for different structure of turbulence. The results of numerical simulations were compared with the primary velocity distribution measured in the laboratory channel. These comparisons show that the model predicts the velocity field reasonably well.

1. Introduction

An important feature of most rivers is a two-stage cross-section consisting of a deep main channel and shallow flood plains, which are often rough due to vegetation. In these channels flood conditions lead to a complex, 3D flow situation with intensive mass and momentum exchange between the main channel and the flood plains. Therefore the flow structures that occur in these channels are

extremely complex. They arise mainly from boundary-generated turbulence and from free shear layer turbulence. The latter reason appears between the main channel and flood plain, where the depth-mean velocities vary laterally, creating a transverse shear layer.

To describe the velocity field in two-stage channels very advanced mathematical models are developed, like the algebraic stress model (ASM) (see for example Krishnappan and Lau (1986) or Naot, Nezu and Nakagawa (1993)) or the complete Reynolds-stress-transport model of turbulence (see for example Cokljat and Younis (1995)). However, these 3D models require a large number of empirical constants that make them of little use for engineering purposes. For example, equations of the algebraic stress model can be classified into three groups (see Naot, Nezu and Nakagawa 1993):

1. Three momentum equations plus the continuity equation governing the three-dimensional mean motion and mean pressure.
2. Two differential equations for the energy of turbulence and the rate of their dissipation. These equations contain four standard empirical coefficients, two additional coefficients and two empirical functions to introduce anisotropic eddy viscosity in transvers directions.
3. Six algebraic (semi-empirical) equations representing the anisotropy of turbulence stresses in terms of the turbulent energy, dissipation rate, and mean velocity gradients. These equations introduce additionally, four empirical functions and two coefficients.

These six differential equations and six algebraic equations are quite complicated. They require eight empirical constants and five empirical functions. Thus, they are not useful for engineering purposes. It is very difficult to understand the roles of all empirical coefficients involved in the models. Then, applying any calibration procedure for these models is almost impossible, and in turn, using these models for other channels is questionable. Engineers need a model that is easy to understand, simple to calibrate and reasonably good.

The three dimensional turbulent models for compound channel flows fulfilled all engineering demands are rather scarce. The main goal of this paper is to present a new model that can be accepted by engineers. The model is based on 3D generalization of widely known MLH of Prandtl. This generalization of Prandtl's mixing length concept consists in transition from scalar mixing length to mixing length second rank tensor. This generalization is related only to turbulence shear stresses and was developed by Czernuszenko and Rylov (2000). This approach allows mixing length to vary between different space directions. It is shown how to define the mixing length tensor for compound channels and relate it to the turbulent stress tensor. The numerical simulation results of primary velocity distributions show that they are very close to those from measurements.

2. Basic Hydrodynamics Equations

Three-dimensional, steady and uniform turbulent flow in compound channels is governed by the Reynolds-averaged Navier-Stokes equations. The continuity and momentum equations for incompressible turbulent flows may be written in the Cartesian tensor notation as follows:

- continuity equation

$$\frac{\partial U_i}{\partial x_i} = 0, \tag{1}$$

- momentum equations

$$U_j \frac{\partial U_i}{\partial x_j} = -\frac{1}{\rho}\frac{\partial P}{\partial x_i} + F_i - \frac{\partial}{\partial x_j}\left(\overline{u_i u_j} - \nu \frac{\partial U_i}{\partial x_j}\right), \tag{2}$$

where U_i and u_i are the i-th component of the time average velocity and turbulent velocity, respectively ($i = 1, 2, 3$), P is the pressure, ρ is density, ν is viscosity and $\mathbf{F} = (g \sin\alpha,\ g\cos\alpha,\ 0)$ is a gravity force. A notation of x for horizontal (longitudinal), y for vertical (downwards) and z for lateral coordinates as well as U, V, W for corresponding velocity components will also be used in the paper.

3. Turbulence Model

The turbulent stresses which appeared in Eq. (2), are described by the 3D mixing length hypothesis (MLH) introduced by Czernuszenko and Rylov (2000). This hypothesis assumes that the mixing length is different in different directions, i.e., the mixing lengths create the mixing length ellipsoid (MLE) at any point of flow. The general form of the turbulence stresses reads:

$$-\rho\overline{u_i u_j} = -\left(\frac{2}{3}k\rho + \frac{1}{3}\rho l_{mk}^2 D_{km} S\right)\delta_{ij} + \frac{1}{2}\rho\left(l_{ik}^2 D_{kj} + l_{jk}^2 D_{ki}\right). \tag{3}$$

where l_{ij} is the mixing length tensor (MLT), $\mathbf{D}$ is the deformation rate tensor defined by the formula

$$D_{ij} = \frac{\partial U_i}{\partial x_j} + \frac{\partial U_j}{\partial x_i} \tag{4}$$

and quantity S by the formula (Czernuszenko and Rylov 2000)

$$S = \sum_{i,k}\left|\frac{\partial U_i}{\partial x_k}\right|. \tag{5}$$

Eq. (3) states that turbulent stresses are expressed as the sum of normal and shear stresses. It is assumed that the normal stresses are isotropic, but the

shear stresses can differ for different components. For the open channel flows the right-hand sum in Eq. (5) may be reduced to two terms containing derivatives of streamwise velocities in lateral and vertical directions respectively. The other term, in the sum above, contain the lateral and vertical components of the mean velocity vector and do not exceed 1–2% of the streamwise component.

4. Mixing Length Tensor

4.1. Local Coordinate System (LCS)

The MLT (l_{ij}) in a local coordinate system has a diagonal form, i.e., the tensor has only three non-zero components: l_{11}, l_{22}, and l_{33}. Below, these three components are referred to as l_x, l_y, and l_z, respectively, i.e.

$$l_{ij} = \begin{bmatrix} l_x & 0 & 0 \\ 0 & l_y & 0 \\ 0 & 0 & l_z \end{bmatrix}. \tag{6}$$

To calculate the shear stresses, first the components of MLT must be prescribed in some way. Czernuszenko and Rylov (2002) presented the method of calculating the components of MLT based on a concept of generic mixing length (GML). The slight modified method of calculating these components is presented below.

A generic mixing length, denoted as l_G, is defined in the whole cross-section of a channel. It is assumed that the GML depends only on the distances from the bed and from the water surface. For any point P, the mixing length l_G is defined as follows

$$l_G(P) = (d_1 + d_2) Lw\xi \quad \text{where} \quad \xi = \frac{d_1}{d_1 + d_2}, \tag{7}$$

where d_1 and d_2 are distances from the nearest wall and from the water surface, respectively (see Figure 1) and $Lw(\xi)$ is the function which describes Prandtl's mixing length in a turbulent boundary layer given by Nezu and Rodi (1986)

$$\frac{l}{h} = \kappa\sqrt{1-\xi}\left(\frac{1}{\xi} + \pi\ \Pi \sin(\pi\xi)\right)^{-1} \equiv Lw(\xi), \tag{8}$$

where: κ is the Karman constant, Π is the Coles wake function (wake coefficient). The wake coefficient for open channel flows is close to zero at moderate Reynolds number. It is worth noting that the generic mixing length calculated from Eq. (7) for verticals located in the middle zone of the channel is the same as mixing length calculated from Eq. (8). Close to inclined or vertical walls the water depth is not equal to the sum of d_1 and d_2, therefore these formulae give different values. Based on the generic mixing length the main components of the mixing length tensor can be defined as follows

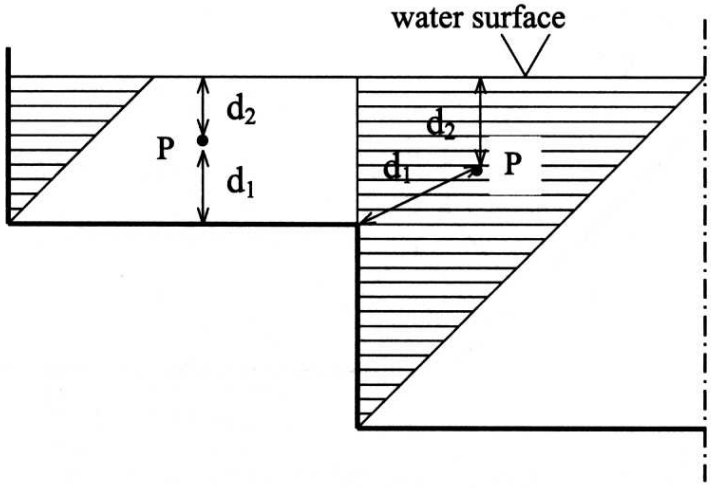

Fig. 1. Definitions of distances d_1 and d_2 in compound cross-section. The marked areas show where the mixing length is reduced compare to Prandtl's mixing length

$$l_x = pl_{3D}\,, \quad l_y = q_y l_x\,, \quad l_z = q_z l_x, \tag{9}$$

where p, q_y and q_z are empirical, positive coefficients. Bearing in mind that Eq. (3) should converge with Prandtl's formula in the middle zone of the channel, it results in constrains on the above mentioned coefficients

$$p^2(1+q_y^2) = 2 \quad \text{for} \quad p < \sqrt{2}. \tag{10}$$

The decomposition of l_G into three main components of the mixing length tensor gives in turn, the decomposition of a sphere with a diameter of l_G into a 3D mixing length ellipsoid with main axes l_x, l_y and l_z. The decomposition means that the scalar mixing length in Prandtl's approach becomes the mixing length ellipse in 2D flow or ellipsoid in the 3D case.

4.2. Global Coordinate System

Equations (7), (8) and (9) enable calculation of the main components of the mixing length tensor in the local coordinate system where the tensor has a diagonal form. Coordinate axes of this system have different directions from those of the global coordinate system in which hydrodynamic equations (1) and (2) are written (LCS and GCS are presented in Figure 2). Therefore MLT components in GCS generally differ from their values in LCS. It depends on the geometry of a channel, whether GCS and LCS coordinate axes actually have the same directions or not. For the central part of the channel these axes are the same, but not for areas close to sidewalls and over inclined walls. For these areas of channels the GCS and LCS are rigidly rotated to each other. The rotation is specified by the angle between

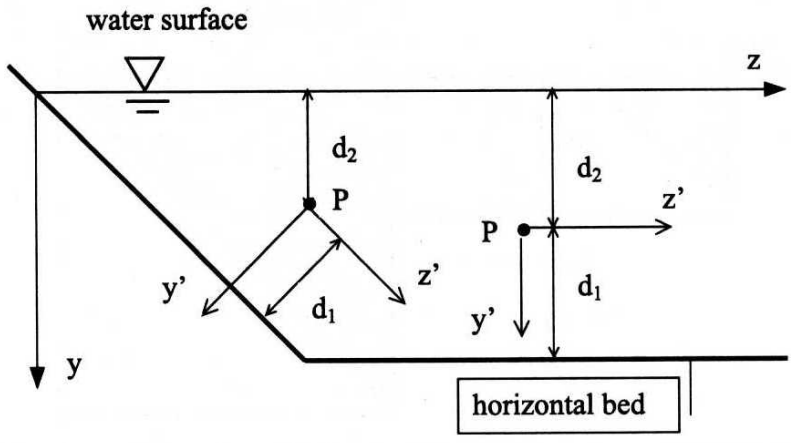

Fig. 2. Local coordinate systems (y', z') defined at point P located over the inclined and the horizontal walls; (y, z) – the global coordinate system; d_1 – distance from a point P to the nearest wall, d_2 – distance to the water surface

the axes of LCS and GCS. This angle differ for different parts of the compound channel. If the angle is equal to α, the transformation will be described by the matrix

$$T = \begin{bmatrix} 1 & 0 & 0 \\ 0 & \cos\alpha & -\sin\alpha \\ 0 & \sin\alpha & \cos\alpha \end{bmatrix}. \tag{11}$$

This means that if a point P has coordinates (x_1', x_2', x_3') in LCS and (x_1, x_2, x_3) in GCS, then the relation between these coordinates is

$$x_i = t_{ij} x_j'. \tag{12}$$

Further in the text, coordinates of points or vectors in LCS as well as the components of MLT in LCS will be primed, but in GCS these quantities will appear without a prime. Please note that so far the coordinates of the local coordinate system have been used without prime. Components of MLT in GCS can be found from the formula (Aris 1989)

$$l_{ij} = t_{ip} t_{jq} l_{pq}'. \tag{13}$$

Combining Eq.(11) with Eq.(13) gives an explicit formula for components of MLH in GCS

$$L = \begin{bmatrix} l_x' & 0 & 0 \\ 0 & l_y' \cos^2\alpha + l_z' \sin^2\alpha & -\dfrac{\sin 2\alpha}{2}\left(l_y' - l_z'\right) \\ 0 & -\dfrac{\sin 2\alpha}{2}\left(l_y' - l_z'\right) & l_z' \cos^2\alpha + l_y' \sin^2\alpha \end{bmatrix}. \tag{14}$$

It is easy to notice that when $l'_x = l'_y = l'_z$ the above formula gives an isotropic MLT.

5. Hydrodynamic Model

Having defined the turbulence model by Eq. (3) and the mixing length tensor by Eq. (14), one can rewrite the basic hydrodynamic equations. Because the continuity equation remain unchanged then only the momentum equations are written below:

$$\frac{\partial U^2}{\partial x} + \frac{\partial VU}{\partial y} + \frac{\partial WU}{\partial z} + \frac{1}{\rho}\frac{\partial P}{\partial x} =$$
$$= g \sin\theta + \frac{\partial}{\partial y}\left(\frac{S}{2}\left(l_x^2 + l_y^2\right)\frac{\partial U}{\partial y} + \frac{S}{2} l_{yz}^2 \frac{\partial U}{\partial z}\right) + \tag{15}$$
$$+ \frac{\partial}{\partial z}\left(\frac{1}{2} S \left(l_x^2 + l_z^2\right)\frac{\partial U}{\partial z} + \frac{S}{2} l_{yz}^2 \frac{\partial U}{\partial y}\right),$$

$$\frac{\partial UV}{\partial x} + \frac{\partial V^2}{\partial y} + \frac{\partial WV}{\partial z} + \frac{1}{\rho}\frac{\partial P}{\partial y} =$$
$$= g \cos\theta + \frac{\partial}{\partial y}\left(2 S l_y^2 \frac{\partial V}{\partial y} + S l_{yz}^2 \left(\frac{\partial W}{\partial y} + \frac{\partial V}{\partial z}\right)\right) + \tag{16}$$
$$+ \frac{\partial}{\partial z}\left(\frac{1}{2} S \left(l_y^2 + l_z^2\right)\left(\frac{\partial V}{\partial z} + \frac{\partial W}{\partial y}\right) + S \left(\frac{\partial V}{\partial y} + \frac{\partial W}{\partial z}\right) l_{yz}^2\right),$$

$$\frac{\partial UW}{\partial x} + \frac{\partial VW}{\partial y} + \frac{\partial W^2}{\partial z} + \frac{1}{\rho}\frac{\partial P}{\partial z} =$$
$$= \frac{\partial}{\partial y}\left(\frac{1}{2} S \left(l_y^2 + l_z^2\right)\left(\frac{\partial V}{\partial z} + \frac{\partial W}{\partial y}\right) + S \left(\frac{\partial V}{\partial y} + \frac{\partial W}{\partial z}\right) l_{yz}^2\right) + \tag{17}$$
$$+ \frac{\partial}{\partial z}\left(2 S l_z^2 \frac{\partial W}{\partial z} + S l_{yz}^2 \left(\frac{\partial V}{\partial z} + \frac{\partial W}{\partial y}\right)\right),$$

where P is the total pressure, i.e., the sum of the pressure resulting from the normal components of the molecular forces and the pressure arising from turbulence; S is defined by Eq. (5); l_x, l_y, l_z and l_{yz} are functions of l'_x, l'_y, l'_z and can be found from Eq. (14).

It is assumed that the considered flow is steady and uniform with constant depth. (rigid lid approximation (Rastogi and Rodi 1978)). The boundary conditions need to be specified along solid boundaries, water surface and upstream cross-section bounding the calculation domain. Since parabolic flows are considered, boundary conditions do not need be given at the downstream end of the calculation domain. The conditions at the solid boundaries were specified using the wall functions technique proposed by Launder and Spalding (1974). According

to this, the conditions are specified at a point near a wall which lies outside the laminar sublayer and satisfies the condition: $30 < u_* y_w/\nu < 100$. The shear stress and velocity at this grid point satisfy the logarithmic portion of the universal law of the wall

$$\frac{u_w}{u_*} = \frac{1}{\kappa} \ln \frac{u_* y_w}{\nu} + A, \tag{18}$$

where u_* = friction velocity, u_w = velocity along the wall, y_w = distance from the wall, ν = molecular viscosity, $A = 5.3$.

Normal velocity components at the solid boundaries and free surface are set at zero. The free surface boundary conditions were specified following the approach of Rastogi and Rodi (1978) which considers free surface to act as a plane of symmetry. Therefore, the gradients of u and v in the y-direction are zeros. The condition at the initial cross section $x = 0$ for longitudinal velocity u was taken along with logarithmic distribution. Components v and w were set as equal to zero.

To solve the above set of equations the numerical parabolic procedure known as the Patankar-Spalding algorithm is used. It solves the set of the above equations for three components of velocity U, V, W and pressure P, at each forward step in a longitudinal direction. Equation for P is derived from (1) to hold it at every computation step. The scheme has HYBRID pattern approximation of convective terms (Leschziner 1980). This scheme gives a reasonably accurate solution for the case considered, as the flow is steady and the numerical grid is aligned with the main flow direction. Due to insignificant secondary velocities the scheme has actually the second order of accuracy.

6. Computational Simulation

6.1. Compound Channel with Vertical Side Walls

The hydrodynamic model Eqs. (1), (15), (16) and (17) together with boundary conditions was applied to simulate the 3D mean stream velocity distribution in compound channel flows. The results of numerical simulations were compared with recently published experimental data by Nezu at el. (1999). The experiments were conducted in a 10 m long and 0.4 m wide tilting flume with compound cross section. Asymmetrical compound open channel was composed of a main channel and a flood plane as shown in Figure 3. The ratio of the flood plain width to the channel width is constant and equal to 0.5. The fully developed turbulent flows were established in the channel for three different rations of depths in flood plain and main channel (h/H), namely: 1/6, 2/7 and 3/8. The Experimental conditions are shown in Table 1.

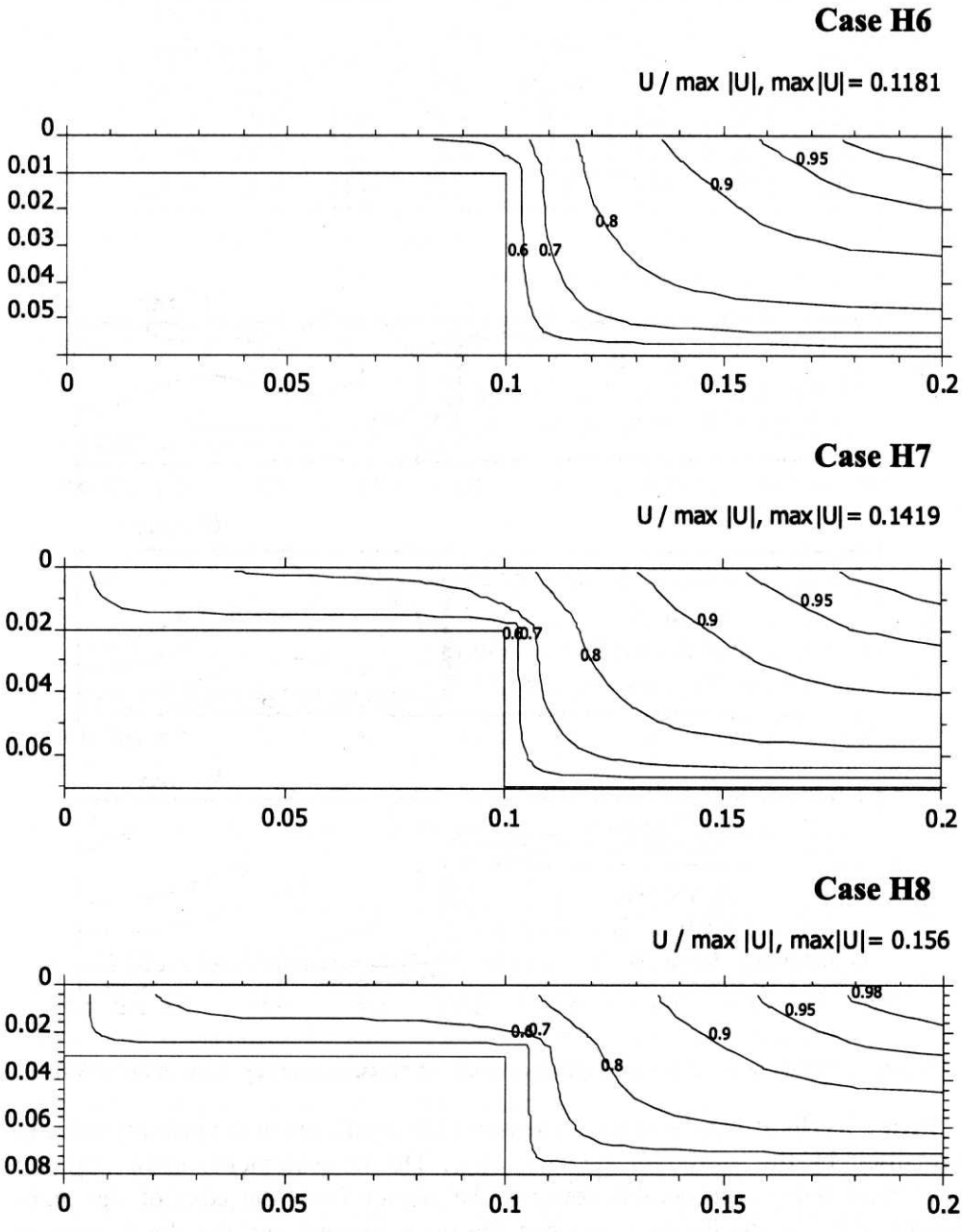

Fig. 3. Contours of primary mean velocity in compound channels with vertical sidewalls: results of numerical simulations

Table 1. Hydraulic conditions data and the numerical simulation results

Case	S slope	H M	h/H cm/cm	U_{mean} m/s	U_{max} m/s	Numerical simulation	
						U_{mean}	U_{max}
H6	1/3000	0.06	1/6	0.10	0.13	0.09	0.118
H7	1/4000	0.07	2/7	0.11	0.15	0.11	0.142
H8	1/5000	0.08	3/8	0.124	0.16	0.12	0.156

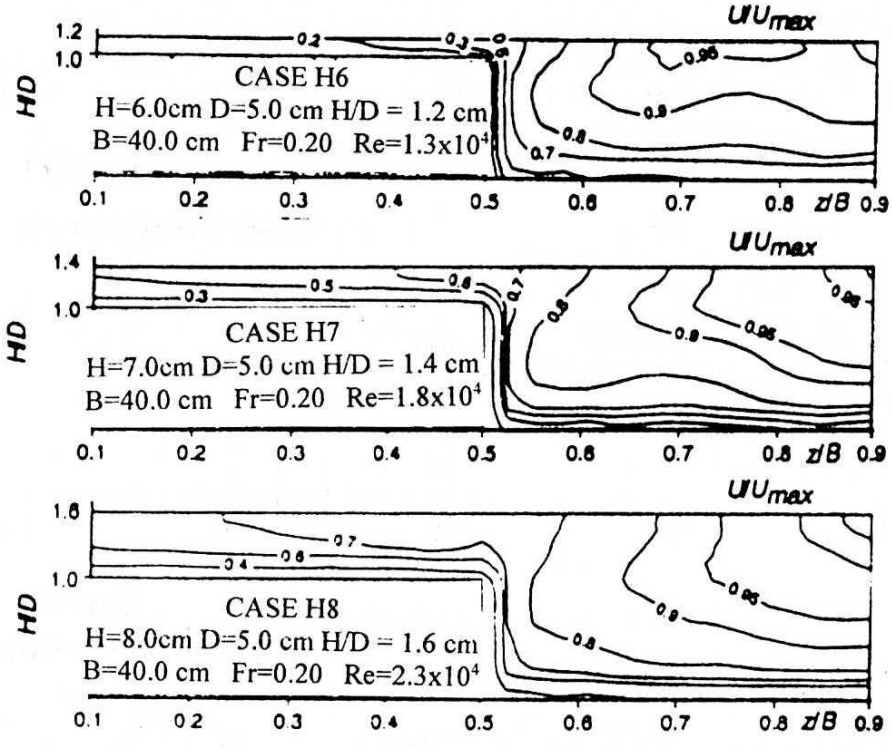

Fig. 4. Contours of primary mean velocity: results of measurements by Nezu et al. (1999)

Figure 3 (H6, H7 and H8) show the isovel lines patterns of the primary velocity normalised by the maximum velocity, U_{max}. The measurements show that the isovel lines bulge considerably towards the corner from the core of the main channel. Also, at the junction between the main channel and the flood plane in case H8, the isovel lines bulge toward the free surface area of the main channel from the corner of the flood plane (Figure 4). The model does not give this kind of behaviour of isovel lines. The model takes into account the influences of the sidewall as well as the junction between the main channel and the flood

plane on the streamwise velocity distribution. These influences are expressed by reduction of the mixing length in suitable areas (see Figure 1). It reduces, in turn, the eddy viscosity in these areas, which allows to increase the velocity gradient. However, this mechanism does not describe these influences with the accuracy desired. To do it, the mechanism of secondary currents must be taken into account. It needs additional information on the distribution of normal turbulent stresses as well as on the distribution of boundary shear stresses. Generally, the normal turbulent stresses are anisotropic, and so far there is not any available model for theses stresses. Neither is there any approach on how to model the boundary shear stresses. Therefore, the secondary currents in this channel are not modelling properly. They are very small and do not influence the prime velocity distribution. Additionally, for this channel equations (15), (16) and (17) are simpler because the mixed mixing lengths are zeros. These resulted in the solution of the whole system of equation and only longitudinal momentum equation are almost the same.

The calculated velocities in the floodplain are much less than those in the main channel. In case H6 the highest velocity in this area is less than 0.6 of the total maximum velocity ($U_{\max}$), for H7 this velocity is generally less than 0.7 $U_{\max}$ and in the case of H8 the highest velocity in the flood plain is less than 0.8 $U_{\max}$. The measurements give the similar numbers, i.e., 0.6, 0.7 and 0.8, respectively. The more global characteristics like the mean velocity and $U_{\max}$ received from numerical simulation are very close to those from measurements. All numerical simulations were performed using the spherical mixing length tensor. This is the simplest model that does not need any calibration procedure and that in the 2D case, reduces to the Prandtl model. It was also assumed that the bed shear stress is constant along the wetted perimeter of the compound cross-section.

6.2. Compound Channel with Inclined Side Walls

The second channel considered is straight with longitudinal bed slope equal to 1.03×10^{-3}. The cross-section geometry of the channel is shown in Figure 5 and some data is displayed in Table 2. The channel has inclined sidewalls 45 degrees and the total width at water surface 52 cm. Measurements of velocity distributions and other parameters are described by Knight el al. (1994).

Table 2. Channel geometry and hydraulic conditions of measurements: h and H are depths in flood plain and main channel, respectively, b and B are widths at the top of the main channel and the water surface, S – longitudinal slope, U^* – friction velocity

Discharge m^3/s	U^* m/s	S slope	h/H m/m	b/B m/m	wall slope degrees	U_{mean} m/s
0.0158	0.023	0.00103	0.04/0.11	0.30/0.52	45	0.468

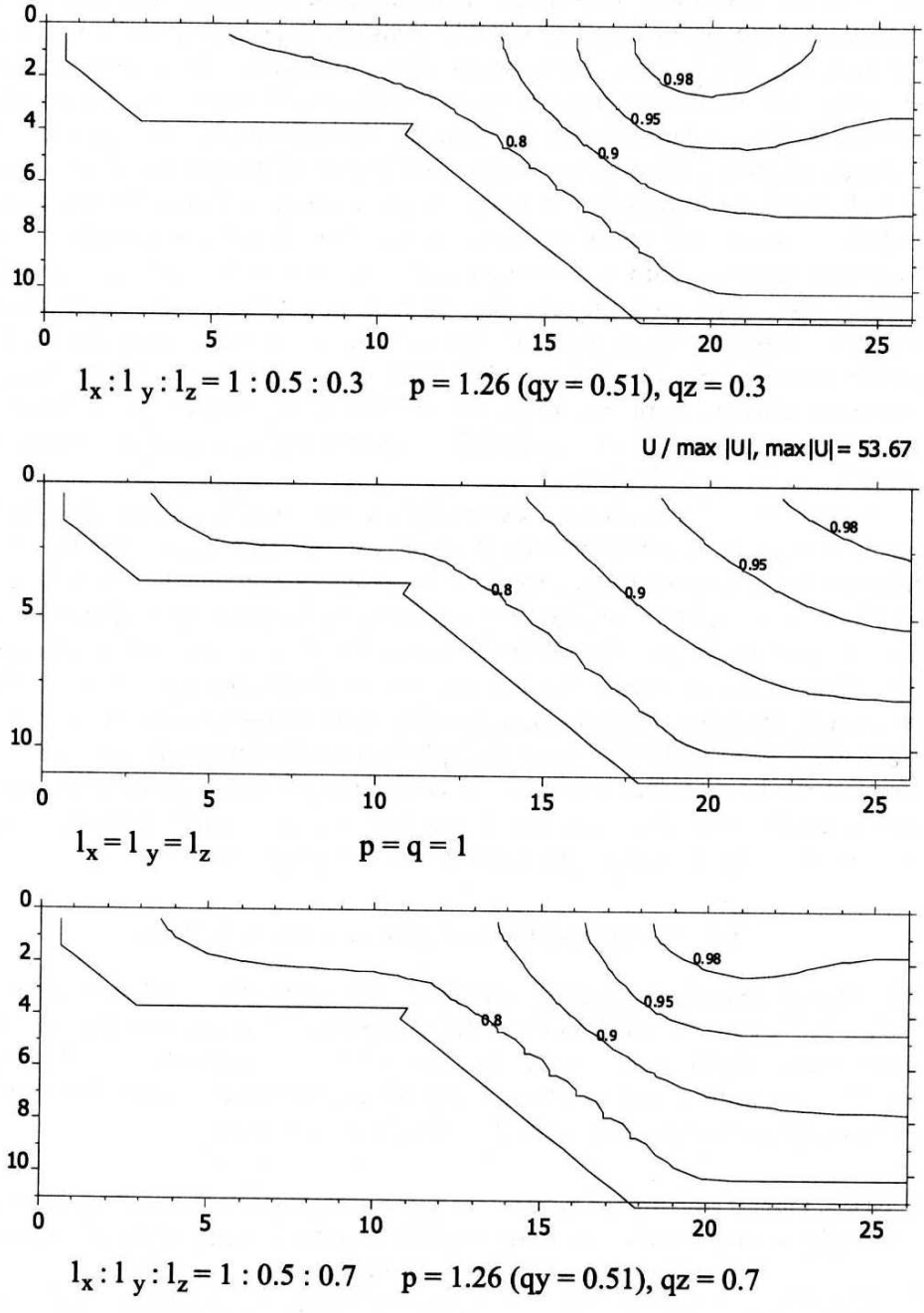

Fig. 5. Contours of primary mean velocity in compound channels with inclined sidewalls: results of numerical simulations

The main objective of the numerical simulations is to show how the model describes the primary velocity distributions in the cross-section of the channel for different structure of turbulence. The structures was defined by the size of the main components of the MLT or in other words by the relative magnitudes of coefficients p, q_y and q_z defined by Eq. (9).

The results of numerical simulations are shown in Figure 5. There are three cases of calculations, namely: – (a): $l_y = 0.5\ l_x$, $l_z = 0.3\ l_x$, – (b): $l_y = l_x = l_z$ and – (c): $l_y = 0.5\ l_x$, $l_y = 0.7\ l_x$. In the case of spherical MLT (Figure 3b) the prime velocity distribution is very regular with logarithmic vertical distribution in the centre of the channel. The U_{max} is located at the water surface in the centre of the channel.

When the mixing length ellipse is narrow in transverse cross-section (Figure 5a, $l_y : l_z = 1.6$), the location of the U_{max} moves in the direction of the side walls. In this case the eddy viscosity in the lateral direction is small, i.e. the lateral transfer of momentum is smaller compared with two other cases. Thus the velocities in the area of flood plain are less than in cases b and c, and the vertical velocity distribution in the centre of the channel is not logarithmic any more. Generally, the transfer of momentum in a lateral direction is retarded.

In the case of wider ellipse (case c, Figure 5c, $l_y : l_z = 0.7$) the transfer of momentum in lateral direction is larger than in the case of narrow ellipse, it also exceeds the lateral transfer in the case of spherical mixing length tensor (case b, Figure 3b). The influence of walls on velocity contour is much greater in case c (Figure 3c) than in the two other cases.

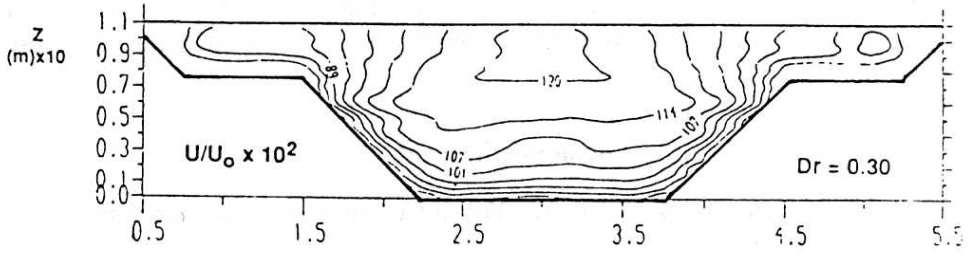

Fig. 6. Contours of primary mean velocity: results of measurements by Knight et al. (1994)

Figure 6 shows the results of prime velocity measurements made by Knight et al. (1994). Velocities in this figure are normalized by the average velocity U_0. Generally, the pattern of velocity contour is not very similar to that received from the simulations. In the main channel, in the area at the water surface the isovel lines bulge towards the inclined walls. This is the result of the influence of both the inclined wall and the water surface. The model does give this kind of

behavior of isovel lines. The model takes into account the influence of the inclined walls as well as the free water surface on the streamwise velocity distribution. The former influence is expressed by reduction of the mixing length in suitable areas. It reduces, in turn, the eddy viscosity in these areas, which affords an increase in the velocity gradient. However, this mechanism does not describe these influences with the desired accuracy. The influence of water surface is expressed by the boundary conditions, which are not suitable in this case.

7. Summary and Conclusions

The 3D MLH is a simple turbulence model that can be used to close the basic hydrodynamics equations for anisotropic turbulence in open channel flows. The model allows us to calculate the streamwise velocity distribution in the compound channel with suitable accuracy for engineering applications. The isovel lines of primary velocity are similar to those received from measurements, with the exception of the area near the water surface in the main channel.

The model is very simple and easy to calibrate. It is particularly simple in the considered channels, i.e., channels with vertical sidewalls or sidewalls with 45 degree inclines. For these channels all mixed mixing lengths in the global coordinate system are zeros. The simplest version of the model, using the spherical mixing length tensor, does not need any calibration procedure. Only the friction velocity and some flow parameters are needed.

A new approach for the estimation of components of MLT is presented. This is based on the idea of generic mixing length and its empirical decomposition into three main components of the MLT. This decomposition should be established based on the procedure of validation and verification of the proposed model. It gives realistically good results when the roughness of bed and sidewalls are close to each other.

Acknowledgement

This work was partially supported by the Polish Committee for Scientific Research under grant 6P04D 020 20.

References

Aris R. (1989), *Vectors, Tensors and the Basic Equations of Fluid Mechanics*, New York.

Cokljat D., Younis B. A. (1995), Second-Order Closure Study of Open-Channel Flows, *Journal of Hydraulic Engineering*, 121, 94–107.

Czernuszenko W., Rylov A. (2000), A Generalization of Prandtl's Model for 3D Open Channel Flow, *Journal of Hydraulic Research*, **38**, No. 2, 133–139.

Czernuszenko W., Rylov A. (2002), Modelling of 3D Velocity Field in Open Channel Flows [will appear in *Journal of Hydraulic Research*], No. 2.

Knight D. W., Yuen K. W. H., Alhamid A. A. I. (1994), Boundary Shear Stress Distributions in Open Channel Flow, [in:] *Physical Mechanisms of Mixing and Transport in the Environment*, Ed. Beven K., Chatwin P. C., Millbark J., J. Wiley.

Krishnappan G. B., Lau Y. L. (1986), Turbulence Modeling of Flood Plain Flows, *Journal of Hydraulic Engineering*, 112 (4), 251–266.

Launder B. E., Spalding D. B. (1974), The Numerical Computation of Turbulent Flows, *Computer Methods in Applied Mechanics and Engineering*, 3, 269.

Leschziner M. A. (1980), Practical Evaluation of Three Finite Difference Schemes for The Computation of Steady-State Recirculation Flows, *Computer Methods in Applied Mechanics and Engineering*, **23**, 293–312.

Naot D., Nezu I., Nakagawa H. (1993), Hydrodynamic Behavior of Compound Rectangular Open Channels, *Journal of Hydraulic Engineering*, 119 (3), 390–408.

Nezu I. Onitsuka K. Sagara Y., Iketani K. (1999), *Secondary currents and bed shear stress in compound open-channel flows with shallow flood plain*, XXVIII Congress IAHR.

Nezu I., Rodi W. (1986), Open-channel flow measurements with a laser doppler anemometer, *Journal of Hydraulic Engineering*, **112** No. 5, 335–355.

Patankar S. V., Spalding D. B. (1972), A Calculation Procedure For Heat, Mass and Momentum Transfer in ThreeDimensional Parabolic Flows, *J. Heat Mass Transfer*, Vol. 15, 1787–1806.

Rastogi A. K. Rodi W. (1978), Predictions of Heat and Mass Transfer in Open channels, *Journal of the Hydraulics Division*, **104**, No. HY3, 397–420.